Use of Particulate Mechanics Concept in Characterizing Soil and Crop Residue Interaction in Tillage

Joash Bryan Adajar, Marolo Alfaro & Ying Chen
University of Manitoba, Winnipeg, Manitoba, Canada

ABSTRACT
Discrete Element Method (DEM) can be used to simulate and assess the performance of a conceptualized soil-engaging tool for tillage applications. In the design of a high-performance soil-engaging tool, it is important to study the interactions of materials involved during tillage: soil, crop residues, and tilling tool. This study focused on crop residues and their interaction with soil. Microparameters of crop residues and soil-residue interface were characterized by back-calculating it using DEM simulations of laboratory experiments. Laboratory experiments performed and simulated were ring shear and direct shear test. The DEM contact model used was linear contact model. Sensitivity analyses on the laboratory test models were performed and it revealed that both particle stiffness (k) and friction (μ) were influential for direct shear test while only μ was influential for the ring shear test. Sensitive microparameters were then thoroughly adjusted until the simulation results matched the laboratory test results. Characterized microparameters can be utilized in improving the reliability of soil-tool-residue DEM models used for tillage simulations.

RÉSUMÉ
La méthode des éléments discrets (DEM) est utilisée pour simuler les performances d'un équipement de labourage conceptualisé. Dans les applications de travail du sol, il est important d'étudier l'interaction entre trois composants, à savoir: sol, résidus de culture et outil de travail du sol. Cette étude s'est concentrée sur les résidus de culture et leurs interactions avec le sol. Les microparamètres des résidus de culture et leur interface avec le sol sont caractérisés par un calcul rétroactif à partir d'expériences de laboratoire simulées. Les expériences de laboratoire réalisées et simulées sont des essais de cisaillement en anneau et de cisaillement direct. Le modèle de contact DEM utilisé était un modèle de contact linéaire. Les analyses de sensibilité ont révélé que la rigidité des particules (k) et le frottement (μ) étaient sensibles au test de cisaillement direct alors que seul le frottement (μ) était déterminant pour les tests de cisaillement en anneau. Les microparamètres sensibles ont ensuite été soigneusement ajustés jusqu'à ce que les résultats de la simulation correspondent aux résultats des tests de laboratoire. Avec une grande prudence, les microparamètres identifiés peuvent être utilisés pour améliorer la performance des simulations de travail du sol.

1 INTRODUCTION

Discrete Element Method (DEM) has been used in modelling soil-tool-residue interactions because of its ability to simulate the occurrence of large displacements, mixing, separation, and flow of particulate materials. The ability of DEM to consider and account soil-tool-residue interactions in microscale level aids in the advancement of agricultural equipment design. Just like any other numerical method, the accuracy of DEM simulations highly depends on the input parameters. This is one of the main difficulties of DEM because there is not a lot of common laboratory experiments that can measure the micromechanical model parameters that characterize the particulate behavior of materials. These particle-based parameters (microparameters) needed for a DEM model cannot be directly correlated to the continuum-based parameters (macroparameters) that most laboratory experiments measure. Also, due to limits in computing ability, representing the actual particle geometry and distribution of a particulate material in a DEM model is challenging (Shmulevich et al. 2009). In order to compensate for the difference in particle geometry considered in the model and absence of a quantitative method of measuring microparameters, a microparameter calibration process of matching the laboratory test simulation results to the ones obtained from the actual test is necessary.

In designing an effective equipment for tillage, it is important to study the interactions between soils, crop residues, and tilling tool. This research focused only on identifying the microparameters of different crop residues and their interface with soil. The objectives of this paper are as follows:

- Perform laboratory experiments to measure shear strength macroparameters of crop residues and soil-residue interface.
- Create a 3D discrete element model of the shear tests.
- Calibrate microparameters by matching the results of the simulation and actual experiment.

2 MATERIAL DESCRIPTION

Crop residues of flax, canola, corn, oats, and wheat were collected at the research farm of Agriculture and Agri-Food Canada in Portage La Prairie, located in the west of Winnipeg at the Central Plains Region of the province of Manitoba. The moisture content of the five field residues after air-drying ranges from 14 – 15% (dry basis).

The soil sample was collected in an agricultural field in Manitoba, Canada. It was classified as a sandy loam soil having a composition of 70% sand, 14% clay, and 16% silt. The liquid and plastic limits of the soil sample were 29.6% and 27.7%, respectively (Nandanwar et al. 2017).

3 LABORATORY EXPERIMENTS

In order to characterize the macroscopic shear behavior of crop residue particles and their interface with soil, two laboratory experiments were carried out. Ring shear test (RST) was performed on the crop residue samples to identify their shear strength macroparameter, internal friction angle. On the other hand, direct shear test (DST) was carried out to quantify the interfacial shear strength macroparameter, interface friction angle, between the crop residue and the soil. RST was used for the crop residue because it was observed that the DST is not capable of providing sufficient displacement to induce shearing until failure. For the interface friction angle between the two materials, DST was deemed effective as it gives the advantage of forcing the shear plane to develop exactly at their interface.

3.1 Ring Shear Test (RST)

Bromhead ring shear apparatus by *Wykeham Farrance International* was used for the test. The ring shear device has an inner and outer diameter of 70 mm and 100 mm, respectively. In compliance to ASTM D6467 (*Standard Test Method for Torsional Ring Shear Test to Determine Drained Residual Shear Strength of Cohesive Soils*), all the crop residues were ground to ensure that the equipment would be capable of shearing the material. The materials were placed loosely on the specimen container prior to the compression and shearing stage. The measured dry bulk density upon placement of the material on the specimen container was 220 kg/m^3.

Experimental factor considered for the ring shear test performed was the crop residue type. The five crop residue types are canola, corn, flax, oats, and wheat. Three normal pressures were selected: 12.5, 25, and 50 kPa. Five test replicates were performed for each residue type. The test methodology was based from ASTM D647. Since no standards for conducting ring shear test on field residues were available, the testing standard for soils was adapted to obtain the desired crop residue shear strength macroparameter.

The material was sheared up to a displacement of 100 mm. Stress-displacement relationships for each test run was plotted. Figure 1 shows the stress-displacement relationships obtained from one set of ring shear test on flax residues. It can be seen that there was an increase in shear strength when the normal pressure was increased. Also, it was observed that for most test runs, shear stress started to yield constant values after a shear displacement of about 60 mm. Residual shear strength of the material was concluded to transpire at the said shear displacement. Similar stress-displacement behavior was observed when the other crop residues were sheared. Given the resulting residual shear strength and its corresponding normal pressure during shearing, Mohr-Coulomb failure criterion was used in developing a failure envelope. A sample failure envelope, which was derived from the stress-displacement relationships previously shown in Figure 1, is shown in Figure 2. The resulting internal friction angle for each of the crop residues, which was calculated by averaging the results from the five replicates, are summarized in Table 1.

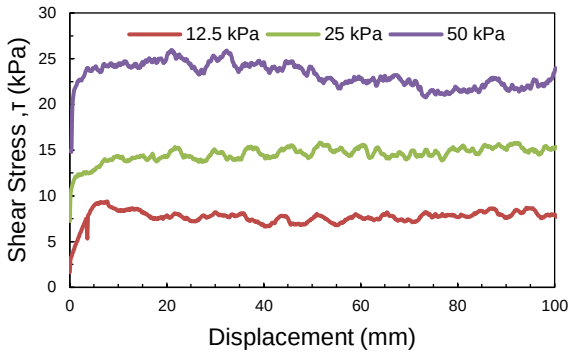

Figure 1. Stress-displacement diagram from RST of flax.

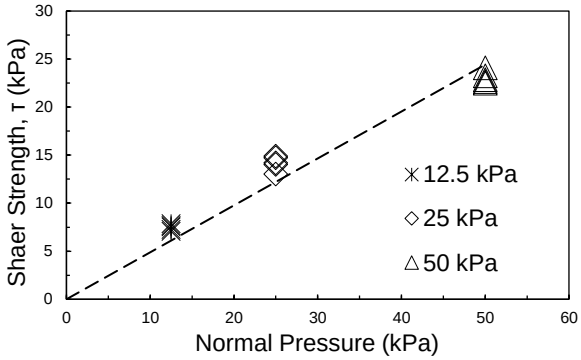

Figure 2. Failure envelope from RST of flax.

Table 1. Summary of measured internal friction angle.

Crop Residue Type	Internal Friction Angle
Flax	26°
Canola	18.9°
Corn	18.8°
Oats	18.9°
Wheat	16.4°

3.2 Direct Shear Test (DST)

A circular shear box having a diameter of 63.5 mm was used for the DST. Crop residues were cut to comply with the maximum size specified by ASTM D3080 (*Standard Test Method for Direct Shear Test of Soils Under Consolidated Drained Conditions*) for the shear box used. A moisture content of 20% was set for the soil sample. Soil sample was positioned at the bottom half while the crop residue was placed at the upper half of the shear box. Shear box set-up can be seen in Figure 3.

Experimental factor considered for the DST performed was once again the crop residue type. Same soil samples prepared at identical conditions were set to be sheared against all the crop residues. It was tested under the normal pressures of 12.5, 25, and 40 kPa. Five test replicates were done for each residue type. The two materials were sheared up to a shear strain of about 15%. Figure 4 shows the state of the materials after shearing.

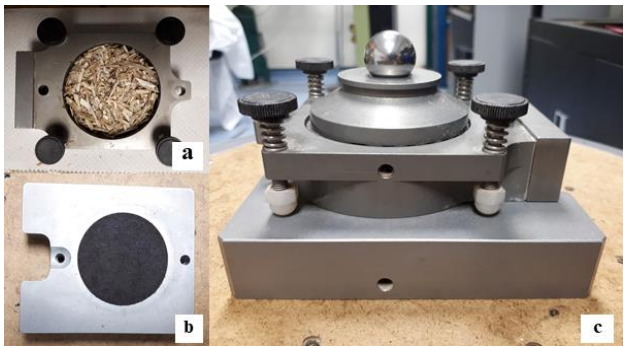

Figure 3. Direct shear box set-up: a) crop residue at the upper half, b) soil at the lower half, and c) final set-up.


Figure 4. Material condition after direct shear test.

Shear strength at failure or the critical-state shear strength considered was the measured shear stress at the end of the test. Figure 5 shows the resulting stress-strain relationships after performing one set of DST on flax and the soil sample. Similar trend on the stress-strain behavior was observed when the other residues were sheared against soil. Figure 6 shows a sample failure envelope which was derived from the stress-strain relationships in Figure 5. Summary of the interface friction angles obtained from all the tests performed, which were calculated by averaging the results from the five replicates, are listed in Table 2. High friction angles obtained may be attributed to the embedment of some crop residue particles on the soil layer as this is inevitable in shearing two different materials. Existence of some fibers and high aspect ratio of crop residue particles may have also increased the shearing resistance.

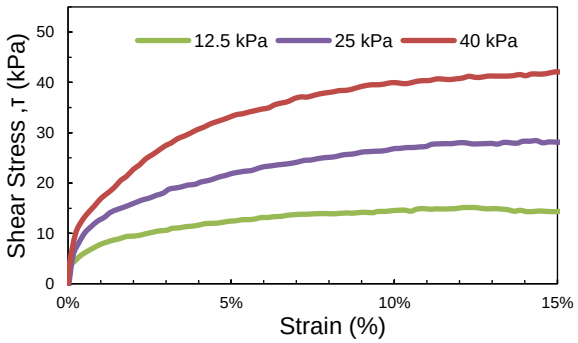

Figure 5. Stress-strain diagram from DST of flax and soil.

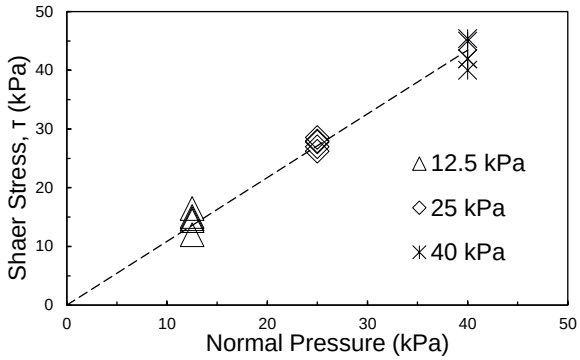

Figure 6. Failure envelope from DST of flax and soil.

Table 2. Summary of measured interface friction angle.

Crop Residue	Soil Sample	Interface friction angle
Canola	Sandy Loam	43.6°
Corn	Sandy Loam	44.4°
Flax	Sandy Loam	47.4°
Oats	Sandy Loam	41.3°
Wheat	Sandy Loam	41.6°

4 NUMERICAL SIMULATION

Discrete element modelling was done using the software "*Particle Flow Code in Three-Dimensions* (PFC3D)." Basic assumptions for the particle-flow model used in PFC3D are as follows (Itasca 2015):

- Particles are considered rigid bodies wherein its assumed shape is spherical. Particles' arbitrary shapes can be created by clumping these spherical particles together.
- Soft-contact approach governs to describe the physical interaction of the contacts that allows overlaps to occur between particles.
- The extent of these overlaps at infinitesimally small contact areas are used to calculate the corresponding contact forces through force-displacement laws.
- Bonds can be assigned at contact points.

Granular behavior of materials, like soil, can be best defined by the soft-contact approach (Cundall et al. 1979). Interaction at contacts that defines the movement of and forces applied on particles are governed by particle-interaction laws called as contact models in PFC3D. Contacts models that were explored in this paper are the linear contact model and linear parallel-bond model. Linear contact model was used to describe the interaction between crop residues. Sadek et al. (2011) used a similar contact model to describe shearing interaction between biomaterials, like hemp fibers and cores. On the other hand, linear parallel-bond model was used to characterize the behavior of the particles of sandy loam soil. This model gives the advantage of assigning bonds at the contacts that represent the cohesive nature of agricultural soil (Nandanwar et al. 2017).

4.1 Ring Shear Test (RST)

4.1.1 Material Vessel

The ring shear device was modelled using four walls. Two cylindrical walls having diameters similar to the inner and outer diameters of the actual ring shear device were generated to enclose the specimen horizontally. While for the vertical confinement, another two walls were created for the lower and upper platen. A 3D-modelling software was used to include serrations on the upper and lower platen, and a friction coefficient of 1 was assigned for both walls. This was done for a proper interlock between the wall and particles in order to ensure particle-particle shearing. A friction coefficient of 0 was assigned at the two cylindrical wall enclosures as the friction of the walls can be considered negligible (ASTM D6467). Sadek et al. (2011) used a similar set of friction coefficients for the vessel walls in shear test simulations using DEM.

4.1.2 Generating Material Particles

Spheres of uniform particle size of 2 mm diameter were selected to represent the crop residue. Bigger particle size was considered because using the same particle size and distribution with the experiment will result for a greater number of particles. It is common for DEM simulations to increase the particles size for it to have a reasonable test runtime because having a large number of particles will require more intensive computations. A total of 9,680 particles were generated and was set to fall with gravity into the material vessel. Considerably low friction was assigned to the material at first to ensure good packing assembly (Mei 2017). Proper microparameters were assigned at a later part before the compression and shearing stage. Particles were then allowed to settle and the system was cycled until it reached a state of equilibrium wherein the average ratio of the unbalanced forces over the sum of all the forces acting in the system is less than 1e-3.

4.1.3 Microparameters

Microparameters associated with the linear contact model are particle normal stiffness (k_n), particle shear stiffness (k_s) and friction coefficient (μ). To decrease the number of parameters to be calibrated, k_n to k_s ratio was assumed to be 1 (Coetzee et al. 2009). Henceforth, due to k_n and k_s being equal, the term particle stiffness will be used to define the value assigned for the two parameters. Sensitivity analysis was done for the particle stiffness and friction coefficient to see how they affect the resulting residual shear strength in the simulations. Base values and their ranges to be tested for the sensitivity analysis are given in Table 3. The chosen base value for the particle stiffness has the same magnitude as the calibrated particle stiffness of hemp core and fiber reported by Sadek et al. (2011). Sadek et al. (2011) used a particle friction coefficient of 1 but the base value for the sensitivity analysis was deliberately reduced to ensure that shearing will occur between particles. Using a particle friction coefficient of 1, which is similar to the wall friction assigned, may lead for the shear plane to develop between the walls and the particles and not between the particles themselves.

Table 3. Values tested for sensitivity analysis.

Parameters	Units	Base Value	Range
Particle Stiffness (*k)*	N/m	7.5e4	7.5e2 – 1e5
Friction (μ)	-	0.1	0.025 - 0.75

Other microparameters to be considered were the local and viscous damping coefficients. Local damping is expected to be assigned for quasi-static simulations while viscous damping is for dynamic simulations (Itasca 2015). A value of 0.7 and 0 were assigned for the local and viscous damping coefficients, respectively. Similar damping coefficients were reported by Nandanwar et al. (2017) and Coetzee et al. (2009) in their quasi-static simulations of laboratory experiments.

4.1.4 Testing Proper

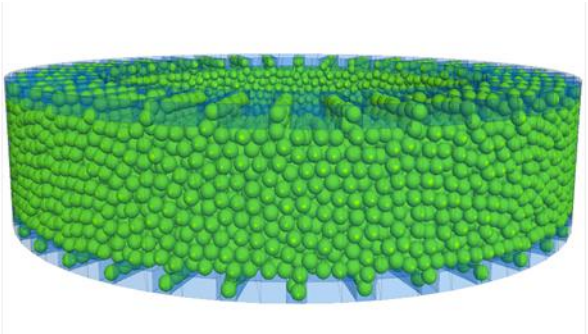

Figure 7. Ring shear test set-up in PFC3D.

Figure 7 shows the ring shear test set-up as modelled in PFC3D. For the compression stage, a *servo* mechanism was assigned to the upper platen in order to apply the designated normal pressure on the material. The *servo* mechanism subroutine allows the program to instantaneously adjust and regulate the translational velocity of the wall so that it can maintain a constant magnitude of applied force throughout the test. Once no succeeding vertical displacement on the upper platen was observed, the bottom platen and the cylindrical walls were rotated clockwise to commence the shearing stage. A subroutine was set to measure the torque at the upper platen and convert it to the corresponding shear stress that is mobilized throughout the test.

4.1.5 Simulation Results

Results of sensitivity analysis indicated that the particle friction coefficient was more influential compared to the particle stiffness. A sudden increase in residual shear strength was observed when the particle stiffness was increased from 7.5e2 to 2.5e3 N/m (Figure 8). Further increase in particles stiffness resulted in minimal to no changes in the residual shear strength. Based on Figure 9, changes in residual shear strength were more prominent when the particle friction coefficient was varied.

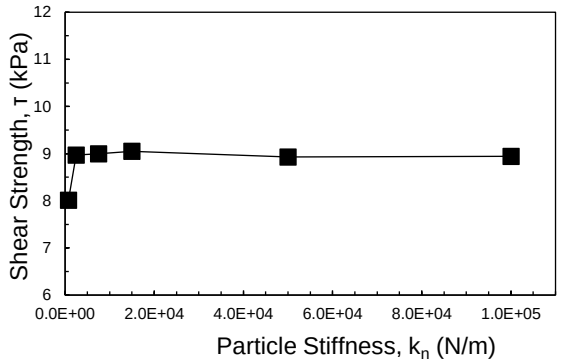

Figure 8. Influence of particle stiffness on RST model.

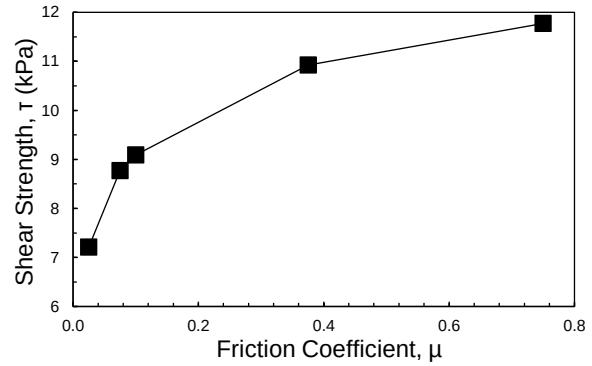

Figure 9. Influence of friction coefficient on RST model.

Microparameter, μ, was chosen for calibration. Since it was observed that minimal to no changes occurred when varying particle stiffness, the base value for the particles stiffness was decreased to 7.5e3 N/m, one magnitude lower than the base value, to shorten the runtime. The calibrated friction coefficient for flax and wheat were 0.425 and 0.025, respectively. For canola, corn, and oats, the calibrated friction coefficient was 0.05.

Stress-strain relationships obtained from performing ring shear test on flax residues are shown in Figure 10. Results obtained from both the actual experiment and numerical simulation are shown in the figure. The simulated stress-strain behavior has good comparison with the measured one. It can be observed that the model was able to simulate the increasing shear strength of the material brought about by the increase in normal pressure. The slight difference that can be seen was that the model was not able to simulate the occurrence of the peak shear strength when the sample was sheared at 12.5 kPa normal pressure. This may be attributed to the difference in particle shape used. The simulation used spherical particles of uniform size that caused for particle rearrangement to be easier compared to the actual residue particles that have a high aspect ratio and was more of cylindrical in shape. Comparison of the failure envelopes derived from the stress-strain curves in Figure 10 is shown in Figure 11. Computed internal friction angles from ring shear test simulations of different crop residues are shown in Table 4. Good agreement can be concluded when comparisons were made with the measured values as the computed relative errors were all less than 2%.

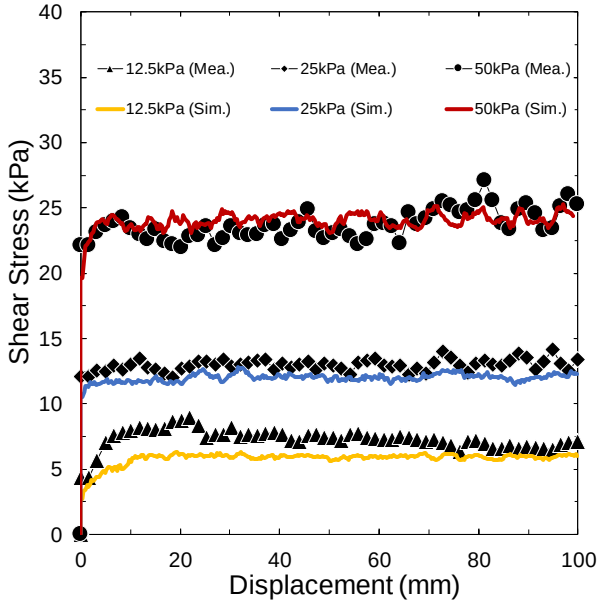

Figure 10. Stress-displacement diagram from both the simulated and actual RST of flax.

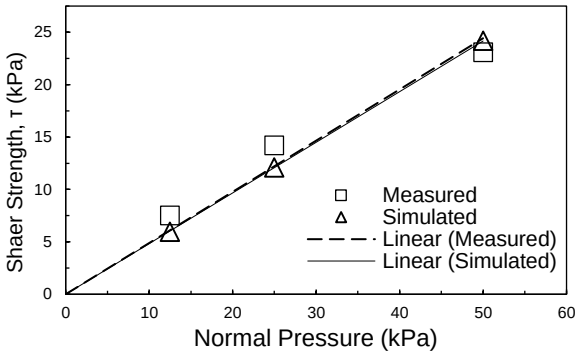

Figure 11. Derived failure envelopes for shearing flax.

Table 4. Comparison of measured and simulated internal friction angles of crop residues.

Residue	Internal Friction Angle		RE(%)
	Measured	Simulated	
Flax	26°	25.8°	.77
Canola	18.9°	19°	.53
Corn	18.8°	19°	1.06
Oats	18.9°	19°	.53
Wheat	16.4°	16.7°	1.83

4.2 Direct Shear Test (DST)

4.2.1 Material Vessel

Four walls were used to model the direct shear box. Two cylindrical walls, having similar diameters and heights to the actual equipment, were used as horizontal enclosures for the upper and lower half of the shear box. Two disks were also generated to represent the bottom and top covers, which were then used to apply vertical pressure.

To mimic the smooth sidewalls of the shear box, a friction coefficient of 0 was assigned to the cylindrical walls. The serrations and roughness of the bottom and top covers were then represented in the model by assigning a friction coefficient of 1 to both the bottom and top disks.

4.2.2 Generating Material Particles

Spherical particles having a uniform diameter of 2 mm were used to represent both the soil and crop residue. Considerably low friction was initially assigned for the soil particles to ensure a compact arrangement. A total of 6,523 soil particles were generated and were set to fall with gravity. It was compressed to guarantee that no further compression by rearrangement of soil particles will govern at the later stages of the simulation and to mimic the compaction made in the actual experiment. A wall was then generated at the center of the box before generating residue particles to avoid mixing of the materials. A total number of 7,845 crop residue particles were then generated and were set to fall with gravity until it reached an equilibrium state.

4.2.3 Microparameters

Initial microparameters assigned for the crop residue particles were similar to what was calibrated from the ring shear test. Microparameters used for the parallel-bond model of soil particles are shown in Table 5. Nandanwar et al. (2017) calibrated these microparameters by performing PFC3D simulations of triaxial test on the same soil sample used in this research.

Table 5. Soil microparameters (Nandanwar et al. 2017)

Parameters	Units	Value
Particle Normal Stiffness (k_n)	N/m	5.4e3
Particle Shear Stiffness (k_s)	N/m	2.57e3
Friction (μ)	-	.7
Bond Normal Stiffness ($\bar{k}_n$)	Pa/m	1.25e10
Bond Shear Stiffness ($\bar{k}_s$)	Pa/m	5.95e9
Bond Normal Strength ($\bar{\sigma}_c$)	Pa	2e4
Bond Shear Strength ($\bar{c}$)	Pa	2e4
Bond Radius Ratio	-	.5

Remaining contact microparameters to be determined were the ones that define the interactions at the soil-residue interface. Linear contact model was assumed to govern at the interface. The surface property inheritance formula stored in PFC3D was used to identify the interface microparameters. With the surface property inheritance approach, linear contact model microparameters between two materials can be identified using the equations:

$$\frac{1}{k_n} = \frac{1}{k_n^{(c)}} + \frac{1}{k_n^{(s)}} \quad [1]$$

$$\mu = \min(\mu^{(c)}, \mu^{(s)}) \quad [2]$$

where the superscripts, c and s, denote that it is the parameter of the crop residue and soil, respectively. The particle stiffness was assumed to behave in series while the smaller value between the friction coefficients was assigned at the interface (Itasca 2015).

4.2.4 Testing Proper

A variation on the laboratory experiment methodology was made in order to make sure that most of the interfacial contacts between the two materials would be positioned exactly along the shear plane. The soil was initially compressed with the designated normal pressure by activating a *servo* mechanism at the lower disk that moves it upwards. Once it stabilized, the *servo* mechanism was turned off and the velocity of the bottom wall was set to zero. The upper disk was then used to compress the residue particles with the same normal pressure. After it stabilized, the disk installed previously at the center that separates the upper and lower half of the shear box was removed. Minimal rearrangement of particles governed along the shear plane to create the contacts at their interfaces, and small vertical displacements were observed from the two materials after stabilization. Shearing stage was then initiated by moving the cylindrical and disk wall at the lower half of the shear box. This process was done so that most of the measured forces during the shearing stage are contributed by the interactions at the interface of the two materials. It was sheared up to 15% strain similar to the experiment. The final state of the model after the shearing stage is displayed in Figure 12. To measure the shear stress experienced by the material, the total horizontal force applied on the right half of the upper cylindrical wall was tracked throughout the shearing stage. It was then converted to shear stress by simply dividing the shear force value with the cross-sectional area of the material projected in the vertical direction.

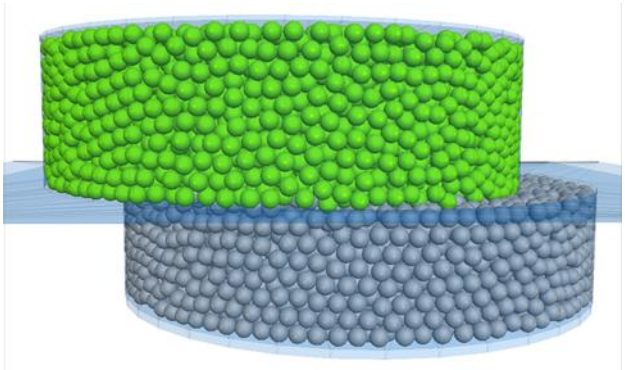

Figure 12. State of the materials after the shearing stage.

4.2.5 Results

After running preliminary direct shear test simulations using the microparameters identified previously, it was observed that results did not match the measured values from the actual experiment. Sadek et al. (2011) and Coetzee et al. (2009) reported that for direct shear test, particle stiffness is as influential as friction coefficient on the resulting shear strength. This is in contrast with what was observed with the ring shear test where varying particle stiffness was not influential to the results at all. Since no calibration of crop residue particle stiffness was done during the simulations

of ring shear test, this situation gave the researcher the opportunity to calibrate it using direct shear test simulations. Sensitivity analysis of the direct shear test model on crop residue particle stiffness and friction coefficient was performed to verify if the findings reported by Sadek et al. (2011) also governs in the model developed. For the sensitivity analysis performed, soil microparameters previously stated were retained while flax residue microparameters calibrated from ring shear test were set as base values. Adjusting the crop residue microparameters simultaneously adjusts the interface contact microparameters due to surface property inheritance. As reflected on Figures 13 and 14, the sensitivity analysis showed that both friction coefficient and particle stiffness were indeed influential, and the particle stiffness was more sensitive for direct shear test compared to its effect in ring shear test simulations. However, it was observed that the particle stiffness became less sensitive as its value increases. For the calibration process, the friction coefficient considered were the ones calibrated from ring shear test. Particle stiffness alone was then calibrated to try and match the measured values. This method was done so that there will be no changes on the friction coefficient and that bulk of the calibration process was dependent on the particle stiffness. This will result for parameters that are still valid for the ring shear test simulation of crop residue particles since it was only dependent on the friction coefficient.

The final crop residue microparameters obtained after the calibration process are summarized in Table 6. Table 7 shows the resulting soil-residue interface microparameters computed using the surface property inheritance approach.

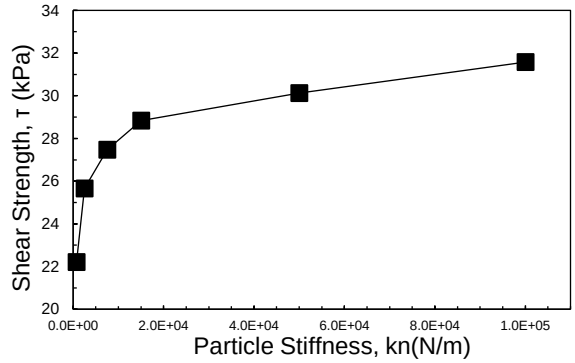

Figure 13. Influence of particle stiffness on DST model.

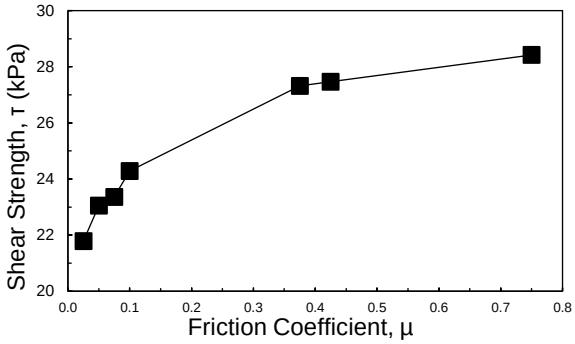

Figure 14. Influence of friction coefficient on DST model.

Stress-strain relationships for both the measured and simulated direct shear test of flax residues and sandy loam soil are shown in Figure 15. Good congruence of the graphs can be observed at higher strains where the shearing is at its critical-state. At lower strains, it can be observed that the shear strength of the simulated ones increases at a higher rate. A similar trend was observed by Hartl et al. (2008) in their direct shear test simulations. The simulated material also reaches critical-state at lower shear strains. This may be due to the increase in the particle size and uniformity of particle shape used that causes rearrangement and critical-state condition to develop faster as it involves less complicated interactions between particles. Although, this difference observed at lower strains is of minimal concern because the research is more concerned with higher displacements or the critical-state and residual conditions of the materials. Same trends can be observed on the simulated stress-strain diagrams when the other crop residues were sheared against soil. Corresponding failure envelopes derived from shearing flax against soil are shown in Figure 16. A summary of the computed interface friction angles from direct shear test simulations is presented in Table 8. Relative errors in comparison with the measured values are all less than 2%.

Table 6. Crop residue microparameters.

Crop residue	$k_n = k_s$ (N/m)	μ
Flax	1e4	0.425
Corn	5e4	0.05
Canola	5e4	0.05
Oats	5e3	0.05
Wheat	2.125e4	0.025

Table 7. Soil-residue interface microparameters.

Material		k_n	k_s	μ
Crop	Soil	(N/m)	(N/m)	
Flax		7e3	4.1e3	0.425
Corn	Sandy	9.7e3	4.9e3	0.05
Canola	Loam	9.7e3	4.9e3	0.05
Oats		5.2e3	3.4e3	0.05
Wheat		8.6e3	4.6e3	0.025

Table 8. Comparison of measured and simulated interface friction angles

Material		Interface Friction Angle		RE
Crop	Soil	Measured	Simulated	(%)
Flax	Sandy Loam	47.4°	47.7°	.63
Canola		43.6°	43.9°	.69
Corn		44.4°	43.9°	1.13
Oats		41.3°	41.5°	.48
Wheat		41.6°	41.5°	.36

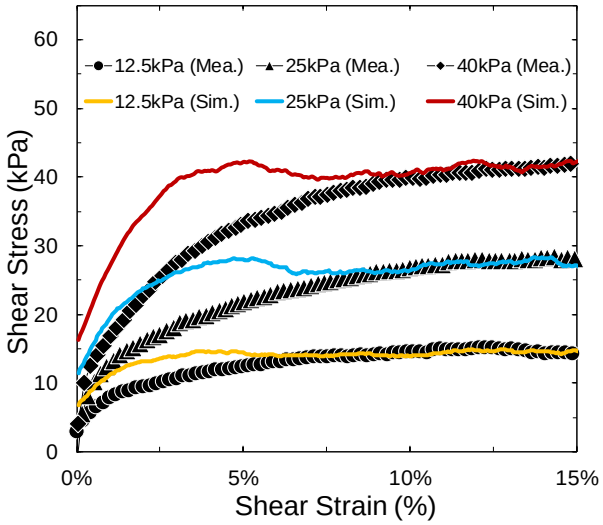

Figure 15. Stress-strain diagrams from both simulated and actual DST of flax and soil.

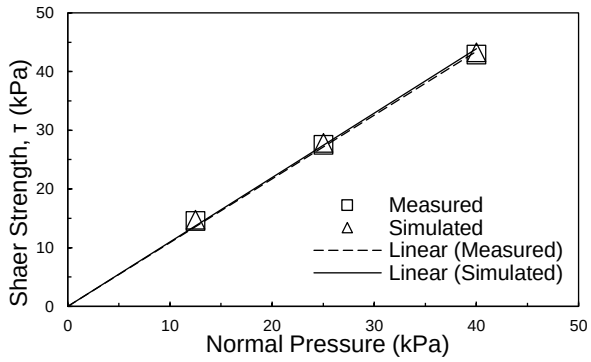

Figure 16. Derived failure envelopes for shearing flax against sandy loam soil.

5 CONCLUSION AND RECOMMENDATION

The calibrated microparameters of crop residues and soil-residue interface were obtained by performing laboratory experiments and simulations of both ring shear and direct shear test. Measured results from RST showed that the crop residues have internal friction angles ranging from 16.4° to 26°. DST results revealed that the measured interface friction angle between the crop residues and soil are from 41.6° to 47.4°. The highest residual and interface friction angle was observed for flax. The relatively higher friction angle values of flax may be attributed to the presence of fibers that improves its shearing resistance.

The discrete element model made using PFC3D was successful in simulating both RST and DST. Linear contact model was able to simulate the behavior of the contacts between crop residue particles as well as its interface with sandy loam soil. Sensitivity analyses identified that different parameters may be influential for different shear tests. Particle friction coefficient (μ) was proven to be sensitive for RST simulations while both particle stiffness (k) and μ were influential for DST. Calibrated μ ranges from 0.025 to 0.425 while particles stiffness ranges from 5e3 to 5e4 N/m. Good comparisons were observed from all the simulated and measured friction angle values which have relative errors less than 2%.

Other mixtures of parameters from numerical modelling can be considered for future studies to be able to better match the stress-strain behavior of the materials. Also, aside from the linear contact model used in this paper, other contact models can be explored to see if it will better simulate the material behavior.

It should be noted that calibrated microparameters should be used with caution as these are only applicable to materials of similar conditions to what was tested in this paper. Different microparameters may govern when analyzing the materials at different moisture levels or different range of confining pressures. Differences in behavior may also arise upon using different particle size, shape, and distribution.

6 REFERENCES

ASTM Standard. 2012. Standard Test Method for Direct Shear Test of Soils Under Consolidated Drained, ASTM D3080, ASTM International, West Conshohocken, PA.

ASTM Standard. 2013. Standard Test Method for Torsional Ring Shear Test to Determine Drained Residual Shear Strength of Cohesive Soils, ASTM D6467, ASTM International, West Conshohocken, PA.

Coetzee, C. J. and Els, D. N. J. 2009. Calibration of Discrete Element Parameters and the Modelling of Silo Discharge and Bucket Filling, Computer and Electronics in Agriculture, *Elsevier*, 5(65):198–212.

Cundall, P. A., and O. D. L. Strack. 1979. A discrete numerical model for granular assemblies, *Géotechnique*, 29(1): 47-65.

Härtl, J. and Ooi, J. Y. 2008 Experiments and simulations of direct shear tests: Porosity, contact friction and bulk friction, *Granular Matter*, 10(4), 263–271.

Itasca. 2015. Particle Flow Code in Three Dimensions, Version 5.0, Itasca Consulting Group, Inc., Minneapolis, MN.

Kotrocz, K. 2017. Numerical Discrete Element Simulation of Soil Direct Shear Test, In the *Proceedings of 31st European Conference on Modelling and Simulation,* Budapest, Hungary.

Mei, C.J. 2017. Determination of Microparameters for Discrete Element. Masters Thesis, University of British Columbia, Vancouver, British Columbia.

Nandanwar, M. and Chen, Y. 2017. Modeling and Measurements of Triaxial Tests for a Sandy Loam Soil. *Canadian Biosystems Engineering*, 59:1–8.

Sadek, M. A. et al. 2011. Characterization of the Shear Properties of Hemp Fiber and Core Using the Discrete Element Method, 54(6), *Transactions of ASABE*, ASABE, 54(6): 2279–2285.

Shmulevich I., Rubinstein D., and Asaf Z. 2009. Chapter 5. Discrete Element Modeling of Soil-Machine Interactions, *Advances in Soil Dynamics*, ASABE, 3:399–433.